Cement & Concrete Composites 34 (2012) 809–818

Contents lists available at SciVerse ScienceDirect

Cement & Concrete Composites

journal homepage: www.elsevier.com/locate/cemconcomp

Effects of activator characteristics on the reaction product formation in slag binders activated using alkali silicate powder and NaOH

Deepak Ravikumar [a], Narayanan Neithalath [b,*]

[a] Department of Civil and Environmental Engineering, Clarkson University, Potsdam, NY 13699, United States
[b] School of Sustainable Engineering and Built Environment, Arizona State University, Tempe, AZ 85286, United States

ARTICLE INFO

Article history:
Received 24 October 2011
Received in revised form 23 March 2012
Accepted 28 March 2012
Available online 4 April 2012

Keywords:
Alkali-activated slag
Compressive strength
FTIR
C–S–H
Silicate polymerization
Silica-rich gel
Salicylic acid–methanol attack

ABSTRACT

The influence of different levels of alkalinity, expressed using the Na_2O-to-source material ratio (n) and activator SiO_2-to-Na_2O ratio (M_s), on the compressive strength development of, and reaction product formation in sodium silicate and NaOH powder activated slag binder systems is discussed. Higher n value mixtures are found to exhibit higher early and later age compressive strengths. An increase in M_s results in reduced early age and slightly increased later age strengths. Compositional coefficients, which are functions of n and M_s are proposed, that relate to the early and later age strengths of the activated slag binders as well as to the shift in the FTIR spectra. The reaction product formation in these systems as a function of the total alkalinity is explained using the shifts of the dominant peak in the FTIR spectra. Fundamental changes in reaction products of powder activated binders as a function of alkalinity is observed. The deductions from the peak shifts are substantiated using the FTIR spectra of the pastes before and after salicylic acid–methanol (SAM) attack.

1. Introduction

Concerns related to greenhouse gas emissions and energy and resource consumption in Portland cement manufacturing has resulted in significant interest on the use of waste and by-product materials as the primary ingredient of structural binders. High volume cement replacement material usage in concrete and the use of cement-less binders are among the prominent strategies that are becoming increasingly accepted to further the cause of materials-related sustainability in the built environment. Cement-less binders generally are alkali-activated systems that use an alkaline activator, typically sodium hydroxide or sodium silicate [1–3], along with a silica-and-alumina rich precursor material to form a final product with properties comparable to that of ordinary Portland cement concrete. Among the precursor materials used, fly ash and ground granulated blast furnace slag have been the prominent ones because of their favorable chemistry (higher amounts of reactive silica and/or alumina species [1–6]) and abundant availability in many parts of the world. Also, since they are extensively used as partial cement replacement materials in concrete, they have been well characterized with respect to their performance in structural concretes.

Alkali activation of slag has been the subject of many studies [7–17]. Caustic alkalis or alkali compounds whose anions can react with Ca^{2+} to form compounds less soluble than calcium hydroxide can act as activators for slag [12,13]. The use of sodium silicate based activators ($Na_2SiO_3{\cdot}xH_2O$ + NaOH) has been found to be ideal to produce desired mechanical properties [3,9,14]. The major reaction product formed as a result of alkali activation of slag is C–S–H gel, which is similar to that formed from Portland cement hydration, but typically with a lower Ca/Si ratio [15–17]. The influence of several parameters relating to the source material and the activator that can potentially influence the reaction kinetics as well as the mechanical and durability properties of the final product has been reported [1,7,14,18]. High amounts of alkalis in the activating medium have been reported to result in early strength gain of activated slag systems [19].

Alkali silicate solutions of varying moduli are generally used as the activating agents. However, the applicability of powder activators, in lieu of the commonly used liquid activators, also need to be evaluated in alkali activated slag binder systems so as to alleviate the concerns related to handling of caustic materials, and facilitate ease of handling. This potentially changes the reaction kinetics, the nature of the C–S–H gel formed, especially with respect to the Ca/Si ratio and the level of polymerization of silicates, and could result in the formation of other reaction products that have a bearing on the mechanical and durability properties of the material. This aspect is considered in this study, where the early and later age reaction

* Corresponding author. Tel.: +1 480 965 6023; fax: +1 480 965 0557.
E-mail address: Narayanan.Neithalath@asu.edu (N. Neithalath).

0958-9465/$ - see front matter © 2012 Elsevier Ltd. All rights reserved.
http://dx.doi.org/10.1016/j.cemconcomp.2012.03.006

products in alkali silicate powder (anhydrous) activated slag binders proportioned using different levels of total alkali loading and activator moduli are analyzed using Fourier-Transform Infrared spectroscopy (FTIR), and related to the mechanical property development and the reaction product stability in such systems. While it is recognized that the powder activated binders do not develop compressive strengths as high as those of waterglass activated mixtures, primarily due to the effects of reduced silica dissolution, strengths in the 30 MPa range, which is the most common strength range for general purpose concrete applications, can be consistently achieved.

2. Experimental program

2.1. Materials

To prepare alkali activated slag pastes and concretes in this study, Type 100 ground granulated blast furnace slag (GGBFS) conforming to ASTM C 989 was used as the starting material. The chemical composition of the starting material is as follows SiO_2 – 36%, Al_2O_3 – 10.5%, CaO – 39.8%, Fe_2O_3 – 0.67%, MgO – 7.93%, Na_2O – 0.27%, SO_3 – 2.1% and loss on ignition – 3%. The silica-to-alumina (SiO_2/Al_2O_3) mass ratio of slag is 3.4, and the basicity coefficient of slag, defined as $(CaO + MgO)/(SiO_2 + Al_2O_3)$, is 1.03. The particle size distribution of slag is such that 95% is finer than 35 μm and the d_{50} is ~10 μm. The X-ray diffraction (XRD) pattern of slag showed that it is amorphous. Combinations of anhydrous sodium silicate powder (>99% sodium silicate and <1% crystalline silica) having a SiO_2-to-Na_2O ratio (or the modulus, M_s) of 1.95, and analytic reagent-grade sodium hydroxide (NaOH) beads were used as the activating agents in this study. The sodium silicate powder has a median particle size of 25 μm and a pH of 12.6 (for a 50% w/v slurry in water). NaOH addition facilitated changing the activator M_s to desired values.

2.2. Mixture proportions

The concrete mixtures were proportioned with approximately 50% of slag + water by volume. River sand was used as the fine aggregate and pea gravel with a nominal maximum size of 4.75 mm was used as the coarse aggregate. The parameters relating to the activator that were chosen to be studied are the Na_2O-to-slag ratio (n) and the SiO_2-to-Na_2O ratio (M_s). The ratio n provides the total amount of Na_2O in the mixture whereas the ratio M_s dictates the proportion of NaOH and sodium silicate powders in the activator. The n values used in this study were 0.05, 0.15 and 0.25, and M_s (mass-based) values ranged from 0.60 to 1.50 in increments of 0.30 (molar-based M_s ranged from 0.62 to 1.55; note that the molar and mass SiO_2-to-Na_2O ratios of sodium silicates are very close since the ratio of molecular masses of SiO_2 and Na_2O is 0.97). For example, if a mixture with an n value of 0.15 and a mass-based M_s of 1.2 is required, for every 1000 g of slag, 150 g of Na_2O and 180 g of SiO_2 is required. Since sodium silicate powder is the only source of silica from the activator, 180 g of SiO_2 can be obtained from 272 g of sodium silicate powder which has a M_s of 1.95. The sodium silicate powder would also provide 92 g of Na_2O. The remaining 58 g of Na_2O (150–92 g) is then obtained by the addition of NaOH. The calculated amounts of the two powder activators were blended with the required amount of slag before mixing. Water-to-powder ratio (w/p) of 0.40 was used for all the mixtures in this study. The powder consisted of slag, sodium silicate and NaOH.

It was observed that paste mixtures proportioned using the desired n and M_s values showed adequate workability (mini-slump flow values in the range of 95–120 mm) even though the higher alkalinity mixtures tend to lose their flowability very quickly, and thus necessitated quick placing and consolidation in the molds. No attempt was made in this study to retard the setting of these binder mixtures, even though such an approach would be necessary for practical applications. The powder was mixed with the aggregates for approximately 30 s after which water was added. The contents were further mixed for 2 min to obtain a uniform mixture. The mixture was then filled in cube molds of 50 mm size and consolidated. Both the paste and concrete specimens were removed from the molds after 24 h, and subjected to moist curing at 23 ± 2 °C and RH > 98%. For the paste specimens to be used for electrical conductivity and Fourier Transform Infrared (FTIR) spectra analysis, samples were prepared by mixing slag and the activating powder so as to obtain the desired n and M_s values, along with the required water in a blender for 2 min. 50 mm × 50 mm × 150 mm prismatic specimens with stainless steel plate electrodes at the ends were used for electrical conductivity determination at various ages. The pastes for the FTIR analysis were mixed in sealed containers.

2.3. Test methods

The compressive strengths of the activated paste or concrete cubes at several ages were determined in accordance with ASTM C 109. Electrical impedance spectroscopy [20,21] was used to determine the electrical conductivity of the activated pastes as a function of time after mixing. Semi-adiabatic calorimetry was used to determine the temperature rise in pastes during early stages of activation.

The samples for FTIR spectroscopy were prepared by mixing approximately 1 mg of sample obtained from carefully sealed specimens, with 300 mg of KBr. The spectra of the precursor materials and the hydrated products at desired ages of curing were obtained using an ATI Mattson FTIR spectroscope in the wavenumber range of 4000–400 cm^{-1} at a resolution of 1 cm^{-1}. Fig. 1 shows the FTIR spectra of the precursor materials, i.e., slag and sodium silicate. The predominant bands in both the spectra correspond to the asymmetric stretching vibration of the Si–O–Si units.

A selective dissolution procedure using salicylic acid and methanol (SAM), also called Takashima's attack [22], was employed on the pastes hydrated for 28 days. This process involved exposing the alkali activated paste to a mixture of salicylic acid dissolved in methanol (1:20). The calcium bearing phases dissolve in this medium, whereas those without calcium form an insoluble

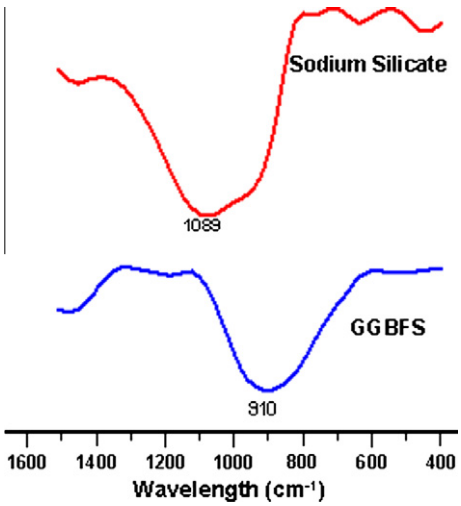

Fig. 1. FTIR spectra of starting materials (slag and sodium silicate powder).

residue. FTIR spectrum of the residue was obtained for comparison with that of the unattacked paste. Morphological analysis was performed using a Scanning Electron Microscope (SEM) operating in secondary mode.

3. Results, analysis, and discussions

3.1. Activator characteristics

In this study, activator in the powder form is used along with slag, and then water is added to this system. In this scenario, it is essential to understand the differences between the properties of binders prepared by: (i) blending the powder activator with slag, and then adding the requisite amount of mixing water, which is desirable from a practical viewpoint, and (ii) adding a premixed activator solution made from the powders (cooled to room temperature) directly, where the desired amounts of sodium silicate and NaOH powders are dissolved in water at room temperature. Sodium silicate with a SiO_2-to-Na_2O molar ratio less than 3.5 is typically soluble in water [23], but has a rather slow rate of dissolution at room temperature. Paste specimens were made using activators of M_s (mass-based) 0.60 and 1.50, at an n value of 0.15 under conditions corresponding to both the above cases. Electrical conductivity of the activated pastes (n = 0.15, M_s = 0.60; w/p = 0.50) as a function of time, for the first 3 days of activation, is shown in Fig. 2. The paste where the activator was blended with the starting material shows higher conductivity at very early times as compared to the paste in which a premixed activator solution was used, and the conductivity drops drastically with time. The higher observed initial conductivity is a result of the increased temperature from the exothermic dissolution of NaOH in water. After around 3 h or so, the conductivities of both the pastes are very similar, as shown in the graph in the inset. Fig. 3a and b depict the compressive strengths of the binder pastes (n = 0.15, M_s of 0.60 and 1.50; w/p = 0.50) where the activator addition was carried out using both the abovementioned methods. It can be noticed from these figures that at ages of 1, 7, and 14 days, the compressive strengths are not significantly influenced by the activator addition method. The electrical conductivity and the compressive strength values show that adding sodium silicate and NaOH as activators in the powder form or by dissolving the powders in water at room temperature and then adding them to the source material produce

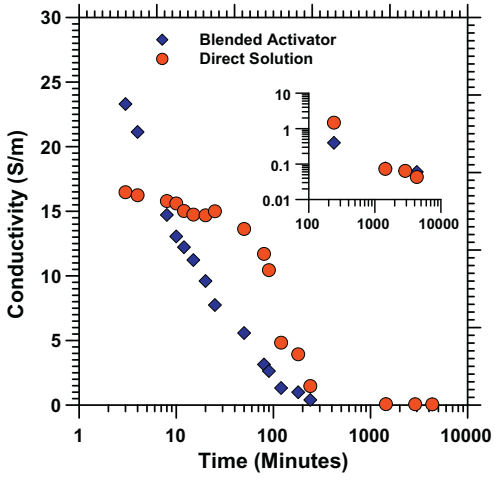

Fig. 2. Electrical conductivity of the alkali activated slag pastes where the activator is directly added as a powder to the source material (blended activator) or added as a solution (direct solution) in which the requisite amounts of activator is dissolved in water (n = 0.15, M_s = 0.60). Similarity of the conductivities after about 200 min is shown in the inset.

comparable results. However, the paste compressive strengths are typically lower than those reported for systems activated using commercial waterglass solutions [24]. This can primarily be attributed to the fact that there is an incomplete dissolution of sodium silicate at room temperature, resulting in a lower amount of reactive silica being liberated into the solution. This changes the reaction product chemistry and composition, as is discussed elsewhere in this paper.

3.2. Temperature and early age strength development

The early-age semi-adiabatic temperature profiles of alkali activated slag pastes proportioned using n values of 0.05 and 0.25 are shown in Fig. 4. It can be immediately noticed from this figure that the peak temperature is significantly higher when the n value is high and activator M_s is low, i.e., at higher Na_2O contents in the mixture. This is because the presence of higher amounts of OH^- enhances the dissolution of slag and the solubility of silica and alumina. For the mixture with a lower n value, the peak temperatures are reached in about 150 min, irrespective of the M_s of the activator. However, for higher n value mixtures, the peak temperatures are reached at around 80 min for the mixture with M_s of 0.60 and at about 120 min for the mixture with M_s of 1.50. The peak temperatures for the lower n value mixtures range from 35 to 40 °C whereas for the higher n value mixtures, they range from 40 to 55 °C. It is seen from this figure that the total alkali content of the mixture (as provided by the n value) is more significant than the activator M_s in dictating the temperature rise and the time to peak temperature. Fig. 4 also shows the semi-adiabatic temperature development curve for an ordinary Portland cement (OPC) paste for comparison. The dormant period which is obvious in the temperature development curve of OPC up to about 300 min is conspicuous by its absence for the alkali silicate powder activated slag systems (though a dormant period is generally noticed for liquid sodium silicate activated slag pastes). The mixtures with lower n and higher M_s values demonstrate lower peak temperatures than the OPC paste. In general, the total heat evolution of alkali activated slag mixtures determined using isothermal calorimetry has been found to be lower than that of OPC mixtures [25].

Fig. 5a and b show the compressive strength development during the first 24 h for the activated concretes proportioned using a w/p of 0.40 and M_s of 0.60 and 1.50 respectively. It can be seen from these figures that there is a considerable strength development in 24 h. For the concretes proportioned using an n value of 0.25 and M_s of 0.60, a compressive strength of about 16 MPa is attained in 24 h. At very early ages (~1–3 h), the compressive strengths are not found to be highly dependent on the n values for a given activator M_s. All the n values are high enough to facilitate the early dissolution of Si and Al species from slag. However, at 24 h, the mixtures with a higher n value show increased compressive strengths, potentially because of the increased slag dissolution under higher alkalinity and the formation of more amounts of reaction products.

3.3. Compressive strength development with moist curing

Compressive strengths of the activated slag concrete specimens that were moist-cured were determined at ages of 1, 3, 7, 14, and 28 days. Fig. 6a–c show the compressive strengths of the activated slag concretes proportioned using n values of 0.05, 0.15 and 0.25 respectively, as a function of the M_s of the activator. These three n values were used to better understand the influence of the amount of alkalis from the activator on the mechanical properties. It can be immediately noticed from these figures that the mixtures having an n value of 0.25 (highest Na_2O content) show the highest

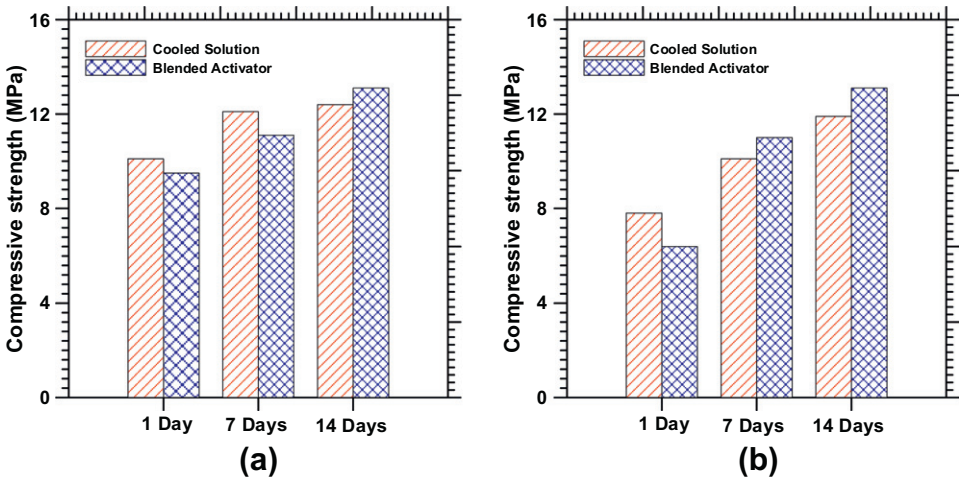

Fig. 3. Comparison of compressive strengths of alkali activated slag pastes when the activator is either blended with the source material or added as a solution in which the requisite amounts of activator is dissolved in water for pastes with n value of 0.15 and activator M_s of: (a) 0.60, and (b) 1.50.

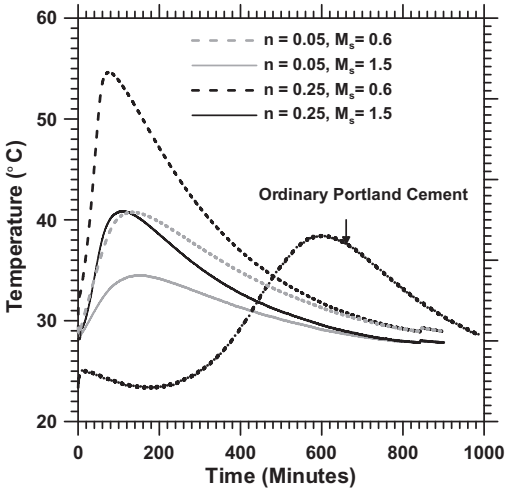

Fig. 4. Early age semi-adiabatic temperature development curves of alkali activated slag pastes with different n and M_s values, and that of an OPC paste for comparison.

compressive strengths at both early (3–7 days) and later (14–28 days) ages. As mentioned earlier, the activation of slag by alkalis is dependent on the efficiency of the alkalis in solubilizing the silica and alumina from slag. It has been suggested that the pH dependent solubility of Si is one of the most important thermodynamical factors influencing slag activation [17]. Higher alkalinity (and consequently higher amounts of OH^- ions) results in increased dissociation of the Si along with the liberation of Ca, and thus increased potential for the formation of more amounts of strength imparting reaction products at early ages. Higher n values (to increase the Na_2O content, more sodium silicate powder is added, which increases both the Na_2O and SiO_2 contents) result in the formation of a silica-rich gel in addition to a Na-incorporated C–S–H gel of low Ca/Si ratio generally reported for activated slag systems. The evidence for this is provided in a later section where the FTIR spectra of these binders are analyzed. There is a significant strength improvement at both early and later ages when the n value of the mixtures is increased from 0.05 to 0.15, but not of the same magnitude when the n value is increased from 0.15 to 0.25. This behavior can be related in part to the limits of dissolution of the powder activator.

When the compressive strengths as a function of activator M_s for a given n value are considered, different trends emerge for early and later ages. Note that the total Na_2O content remains the same for a given n value. At early ages (3 and 7 days), strength decreases fairly linearly with increase in activator M_s for the mixtures with all the three different n values. This is because, at lower M_s values (or

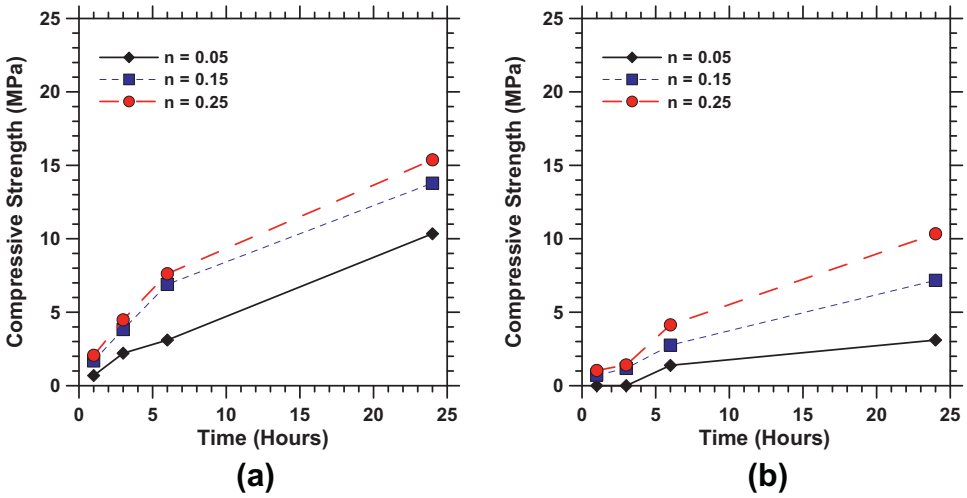

Fig. 5. Early age (up to 24 h) compressive strength of alkali activated slag concretes made with water-to-powder ratio of 0.40 and: (a) M_s = 0.60 and (b) M_s = 1.50.

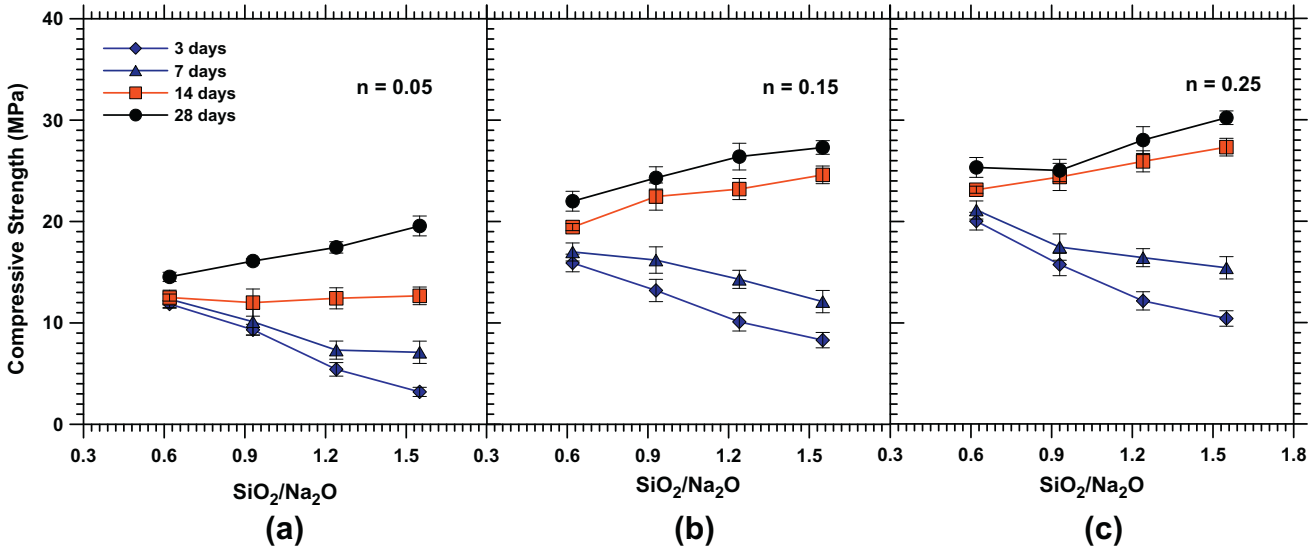

Fig. 6. Compressive strength (3–28 days) as a function of activator M_s (SiO_2-to-Na_2O molar ratio) for moist-cured activated slag concretes proportioned using n values of: (a) 0.05, (b) 0.15, and (c) 0.25 (the error bars indicate one standard deviation from the mean values).

higher Na_2O content of the activator), the higher alkalinity solubilizes the water-impermeable layer on the surface of slag particles [17], leading to a faster reaction rate and formation of reaction products on the surfaces of slag particles. However, at later ages, the trend reverses, and the mixtures made using a higher activator M_s shows higher strengths. This can be partly attributed to the formation of three-dimensional silicate frameworks and sheets at higher M_s, while at lower M_s, formation of two-dimensional silicate chains is preferred. Increased silica polymerization in the C–S–H gel also could facilitate some enhancement in the compressive strengths. The relationship between the compressive strengths of activated concretes at early and later ages and the FTIR signatures of the corresponding pastes are provided in a later section.

3.3.1. Compositional coefficients related to compressive strength

The trends in Fig. 6 clearly show that the compressive strengths of sodium silicate and NaOH powder activated slag concretes exhibit different trends at early and later ages. The early age strength could be thought of as more closely related to the dissolution of slag and the rate of reaction, and thus to the alkali contents of the activator. A compositional coefficient, α, is defined here, which is a function of n, M_s, and the total powder content in the mixture, as:

$$\alpha = \frac{[Na_2O]^2}{[SiO_2] \cdot \text{Total powder}}$$

Increase in n and decrease in M_s were shown in the earlier section to result in better early age compressive strengths. Therefore α can be related to the 3 and 7 day compressive strengths as shown in Fig. 7a. The compositional coefficient α proposed here is: (i) designed specifically to relate to the early age strength of moist-cured activated slag concretes, and (ii) explicitly related to both n and M_s, which are the predominant material design parameters for alkali activated slag concretes. It needs to be noted here that the α values range from 0.01 to 0.30, and its use outside this range has not been tested in this work. The case for $\alpha = 0$ or ∞ does not exist for sodium silicate activated slag concretes because the Na_2O and SiO_2 contents of the activator will never be zero.

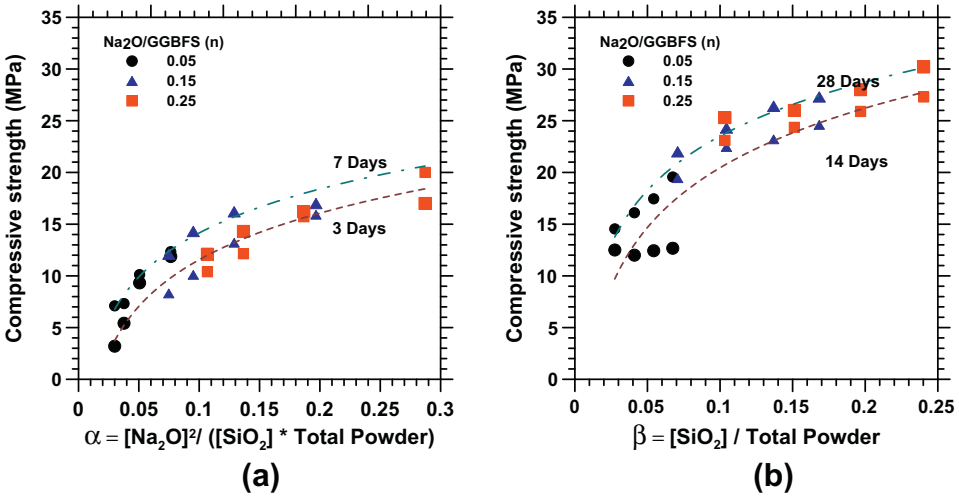

Fig. 7. Compressive strengths as a function of compositional coefficients: (a) early age (3 and 7 day) strengths as a function of compositional coefficient α, and (b) Later age (14 and 28 day) strengths as a function of compositional coefficient β.

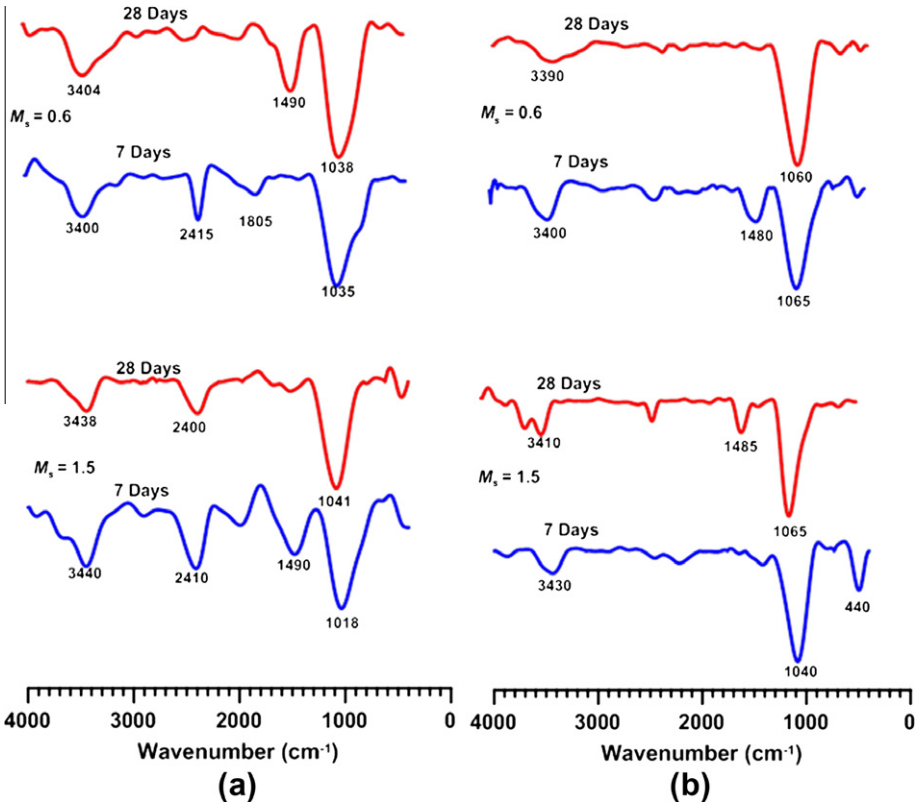

Fig. 8. FTIR spectra of alkali activated slag pastes at 7 and 28 days: (a) n value of 0.05 and (b) n value of 0.25. The corresponding M_s values are shown adjacent to the respective spectra.

The later age strengths can be considered to be mostly dependent on the formation and/or polymerization of silicate structures. Hence a compositional coefficient, β, is used to relate to the later age strengths of the activated concretes, defined as:

$$\beta = \frac{[SiO_2]}{\text{Total powder}}$$

Since the total powder content includes the contents of SiO_2 and Na_2O of the activator along with the slag content, β can be shown to be proportional to M_s. Fig. 7b shows the relationship between β and the later age strengths of activated slag concretes. The limits of β considered in this study range from 0.01 to 0.25. The advantage of both these compositional coefficients is that the early and later age strengths are related to specific individual parameters that implicitly incorporate the M_s and n values. The powder content is used instead of the slag content in these coefficients so that these relationships could be used even in cases where the slag and the activators are inter-ground or blended to produce a binder that only requires the addition of water to set and harden.

3.4. FTIR analysis of activated pastes: reaction product constitution as a function of activator characteristics

Fig. 8a and b represent the 7 and 28 day FTIR spectra of activated pastes with n values of 0.05 and 0.25 respectively, for M_s values of 0.60 and 1.50. The major bands observed between 1000 and 1065 cm^{-1} represent the asymmetric stretching vibrations of the silica tetrahedral. In addition, stretching and deformation modes of OH^- at around 3400 cm^{-1} and asymmetric stretching mode of calcite at ~1490 cm^{-1} are observed. As expected, CH band (at ~3635 cm^{-1}) is absent. CH cannot precipitate in these systems because of its higher solubility as compared to C–S–H and C–A–S–H. It is well known that activation of slag with sodium silicate results in the formation of C–(A)–S–H gel and a hydrotalcite-like phase (co-existing with C–S–H, depending on the MgO content of the slag) as the major reaction products [15,26–28]. The discussions here are limited to the stretching vibration of Si–O–Si units since it can be used as a signature of the constitution of reaction products.

In general, for C–S–H and C–A–S–H systems, the Si–O–Si stretching bands are generally observed at a wavenumber of 950–1000 cm^{-1} [22,29–31], associated with a silica network that is not highly polymerized. However in the FTIR spectra for the alkali silicate and NaOH powder activated pastes shown in Fig. 8a and b, the wavenumbers corresponding to the Si–O–Si peak are observed to be higher, and vary between 1018 and 1065 cm^{-1} depending on the activator alkalinity and the specimen age. The possible reasons for the increase in wavenumber are discussed in detail in the following sub-sections. It needs to be mentioned here that such shifting of the peaks to higher wavenumbers is found to be a characteristic of sodium silicate powder + NaOH activated slag binders. Waterglass (sodium silicate solution) activated slag pastes examined in a companion study revealed the main Si–O–Si stretching peaks in the 970–1010 cm^{-1} range as is common for conventional C–S–H gels from cement hydration, pointing to the fundamental differences in the reaction products between slag pastes activated using solid and liquid sodium silicate activators.

3.4.1. Shift in wavenumber induced by changes in the C–S–H gel

A shift to a higher wavenumber is typically interpreted as the effect of higher Si content in the C–S–H gel (or a lower Ca/Si ratio) [32]. Here, a short discussion is provided as to the potential reasons for this shift based on the changes in C–S–H gel. The alkali activated slag pastes are reported to consist of a lower Ca/Si ratio C–S–H gel (0.6–0.7 for waterglass and 0.9–1.0 for NaOH activated slag pastes) [32,33]. Gels with a lower Ca/Si ratio have a higher

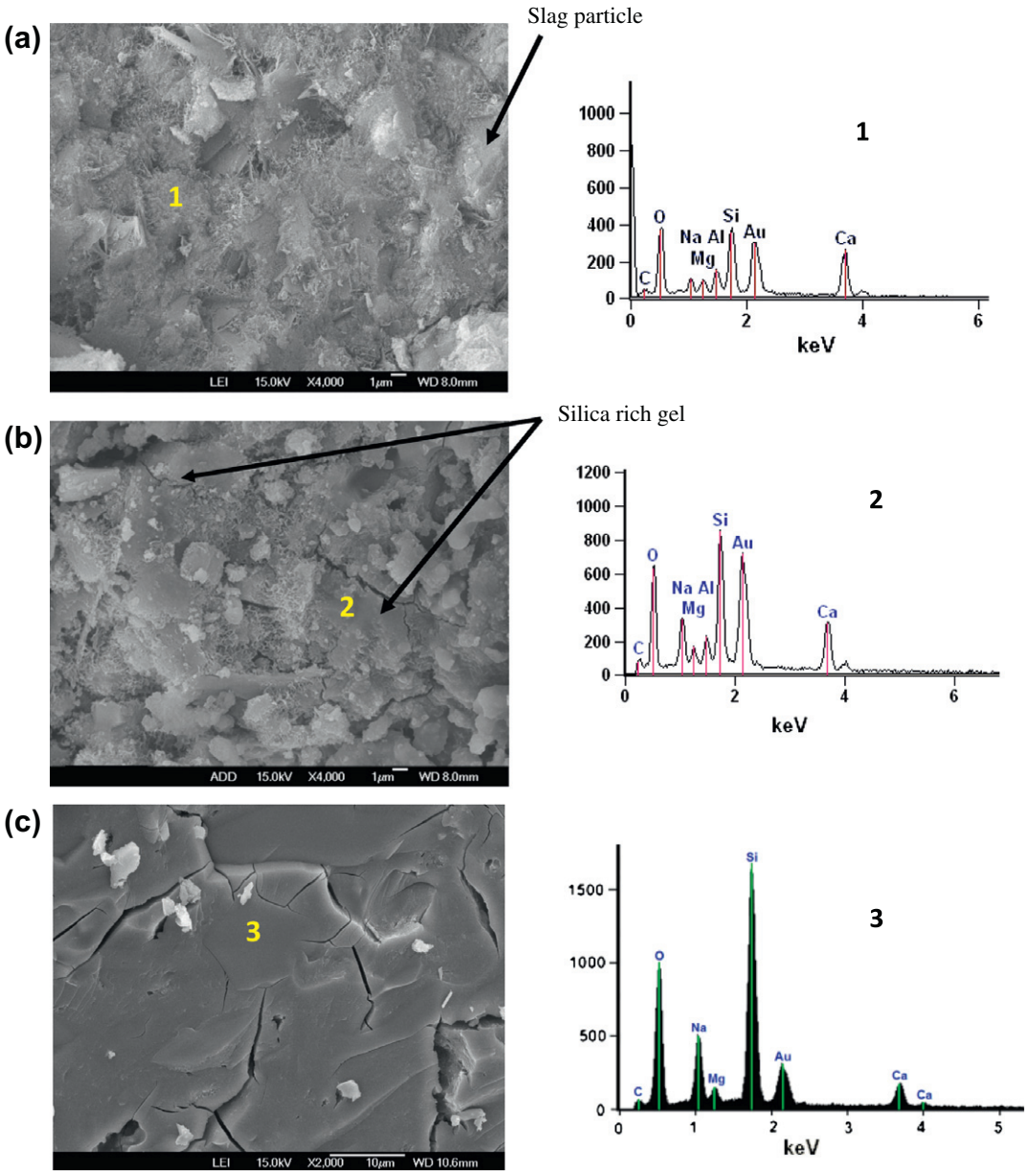

Fig. 9. Scanning electron micrographs of: (a) paste with $n = 0.05$ and $M_s = 1.5$, showing slag particles and reaction products, mostly C–S–H, (b) paste with $n = 0.25$ and $M_s = 0.6$, showing the extensive presence of sodium silicate gel, and (c) NaOH activated glass powder paste showing the presence of smooth sodium silicate gel alone as the reaction product. The EDX spectra at the numbered locations for a low Ca/Si ratio C–S–H gel (a), a silica rich gel containing Na and Ca (b), and a Na-silicate gel (c) are also shown. The activated slag pastes were moist cured for 28 days whereas the glass powder paste was heat cured.

potential to incorporate increased amounts of Na, and the amounts of alkali incorporation in C–S–H gel is almost linearly proportional to the initial alkali content [24]. Thus, the pastes made using higher n values are likely to have an N–C–S–H gel with the Na/Ca ratio approaching that of the maximum limit dictated by the conditions of gel electroneutrality. This, along with the lowering of the Ca/Si ratio, plausibly results in the production of Q^3 silicon, which can cross-link between adjacent silicate chains [33], as opposed to the Q^1 and Q^2 units predominantly found in C–S–H gel from Portland cement pastes [34,35]. An IR absorption band in the 1000–1050 cm^{-1} range as seen in Fig. 8a and b is consistent with the predominance of Q^2 and Q^3 silicates [23]. Some amount of Q^3 silicates in addition to Q^2 silicates have been reported in the C–S–H formed in waterglass and NaOH activated slag systems [32,36].

Another possibility that has been reported to result in an amorphous silicate with a higher degree of polymerization is gel carbonation [32]. While it is known that C–S–H carbonation can occur at higher alkali contents, the FTIR spectra in these figures do not indicate intense carbonation. The carbonate bands found in some of the FTIR spectra can be considered to have occurred during the specimen preparation for FTIR analyses because the thermogravimetric analyses of the 28-day cured (in sealed conditions) samples did not show indications of carbonation.

3.4.2. Presence of a silica-rich gel modifying the FTIR spectra

Another potential reason for the shift of the Si–O–Si band to higher wavenumbers in the powder activated binders could be the extensive presence of hydrated silica-rich gel in the microstructure. The presence of small amounts of sodium silicate gel in waterglass activated slag pastes (M_s of 1.50) has been reported [33]. In the present study, powder sodium silicate of a higher modulus is used as the activating agent. Higher modulus alkali silicates

in solution have a tendency to over-saturate and result in the crystallization of a solid phase which is likely a combination of alkali silicate or meta-silicate hydrates [24]. This cross-links the slag particles, and the amount of cross-linking increases with time. The presence of unreacted sodium silicate in high n value mixtures, where more Na_2O and SiO_2 are present because more sodium silicate powder is used to increase the Na_2O-to-slag ratio (because of incomplete dissolution), also cannot be discounted. This also results in Q^3 silica species being detected that contributes to the shift to a higher wavenumber.

The differences in reaction product morphology between pastes of lower and higher n values are shown in Fig. 9a and b. Fig. 9a shows the scanning electron micrograph of a 28-day old paste made using a n value of 0.05 and M_s of 1.5 (lowest alkalinity). The micrograph shows the presence of some slag particles and the reaction products that are formed. The EDX spectrum indicates a low Ca/Si ratio C–S–H gel with likely Na incorporation. In Fig. 9b, the micrograph of the 28-day old paste made using an n value of 0.25 and M_s of 0.6 (highest alkalinity) is shown. The presence of a smooth silica-rich gel is noticed. The increasing amounts of NaOH added to maintain the selected M_s values of the activator changes the number of network modifying sodium atoms per silicon atom. The structure of the gelatinous silicate phases produced is modified by the presence of Na atoms [23,37]. Since some of the Na ions will be incorporated in the C–S–H gel, either replacing Ca ions to form N–C–S–H gels [24,30] or as charge balancers to compensate the substitution of Si^{4+} with Al^{3+} [29,33,38], the modulus of the thus produced sodium silicate gels will be higher; in other words, the gels will be silica-rich. Higher SiO_2-to-Na_2O ratio of these sodium silicate gels implies decreased number of non-bridging oxygen sites (or more polymerization), thereby preferentially forming Q^3 silicate structures, which shows a higher wavenumber corresponding to the asymmetric stretching vibration of the silica tetrahedral.

The micrograph in Fig. 9a and the FTIR spectra in Fig. 8a shows that in lower alkalinity mixtures (n = 0.05, M_s = 1.5), a modification of C–S–H gel is the likely outcome, with the wavenumbers shifted to around 1030 cm^{-1}. Lower amounts of sodium silicate in these pastes reduce the probability of incomplete dissolution and consequently the amounts of sodium silicate gel. At a higher alkalinity (n = 0.25, M_s = 0.6), Figs. 9b and 8b indicate the presence of a much more polymerized silica-rich gel in the material structure, with the wavenumbers shifting to around 1060 cm^{-1} (note that pure silica shows a characteristic band at 1100 cm^{-1}). Fig. 9c shows the microstructure of pure sodium silicate gel produced from the activation of a silica rich glass powder by NaOH, for comparison. Based on the above discussions, it can be deduced that the use of smaller amounts of sodium silicate + NaOH powder as activator (i.e., lower alkalinity – lower n and higher M_s) leads to the formation of C–S–H gel with a low Ca/Si ratio as the dominant product, whereas the dominant product is likely to be a silica-rich gel at higher activator alkalinities. In the following section, results of salicylic acid–methanol attack (Takashima's attack) is provided to confirm this finding.

3.4.3. Observations from FTIR spectra after salicylic acid–methanol (SAM) attack: influence of alkalinity on reaction product formation

FTIR spectra of the insoluble residues after exposure of the 28-day old activated pastes to salicylic acid–methanol solution, along with the spectra of the unattacked specimens are shown in Fig. 10. The spectra (a) is for the paste made using the activator with the lowest alkalinity (n of 0.05 and M_s of 1.5), spectra (b) for the paste with intermediate alkalinity activator (n of 0.25 and M_s of 1.5), and spectra (c) for the paste with the highly alkaline activator (n of 0.25 and M_s of 0.6). From spectra (a), it can be noticed that the main Si–O–Si peak observed at 1038 cm^{-1} before the attack is non-existent after the attack, and a broad peak at around 905 cm^{-1} makes its appearance. It is known that the C–S–H gel and the other Ca bearing phases are soluble in the test medium. This shows that the low alkalinity paste has a reaction product constitution that is mainly a low Ca/Si ratio C–S–H gel. FTIR spectra before and after SAM attack for an OPC paste, and a NaOH activated Class F fly ash paste are shown in Fig. 11. The OPC paste has C–S–H gel as its major reaction product and has lost all of it after the SAM attack, as seen from the absence of the main Si–O–Si peak, whereas the SAM attack resulted in no change at all for the NaOH activated fly ash paste since the reaction product is exclusively a sodium aluminosilicate (N–A–S–H) gel that does not contain any Ca. It can also be noticed from this figure that the Si–O–Si peak in N–A–S–H gel appears at lower wavenumbers than for the Ca bearing systems (Fig. 8) in which silicates are highly polymerized and/or a silica-rich gel is present.

Spectra (a) of Fig. 10 suggests that the reaction product formed when slag is activated using an activator of lower alkalinity can be considered to be similar to conventional C–S–H gel (see Fig. 9a) that is dissociated by the SAM attack. The case corresponding to the lower alkalinity activator used here does not result in drastic changes in the C–S–H gel, except for the lowering of the Ca/Si ratio and the binding of some Na into the C–S–H gel. An observation of spectra (b) for the paste with intermediate alkalinity activator shows that the main peak, indicative of much more polymerized silicates and sodium silicate gel, is not completely transformed by the SAM attack. The peak is found to broaden as a result of depolymerization and a corresponding decrease in the Si–O–Si bond angle [39]. Higher amounts of insoluble residue were observed after the SAM attack in this case as compared to the paste with the lowest alkalinity, attesting to the presence of a highly polymerized silica rich gel. Spectra (c), corresponding to the highest alkalinity virtually shows no change in the wavenumber

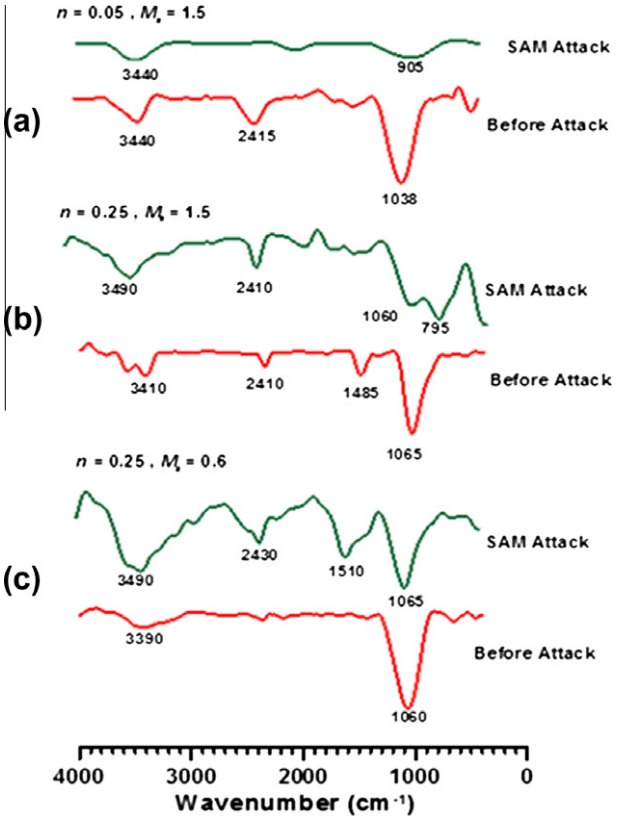

Fig. 10. FTIR spectra of alkali activated slag pastes before and after salicylic acid–methanol (SAM) attack: (a) n = 0.05, M_s = 1.50 – lowest alkalinity; (b) n = 0.25, M_s = 1.50 – intermediate alkalinity; (c) n = 0.25, M_s = 0.60 – highest alkalinity.

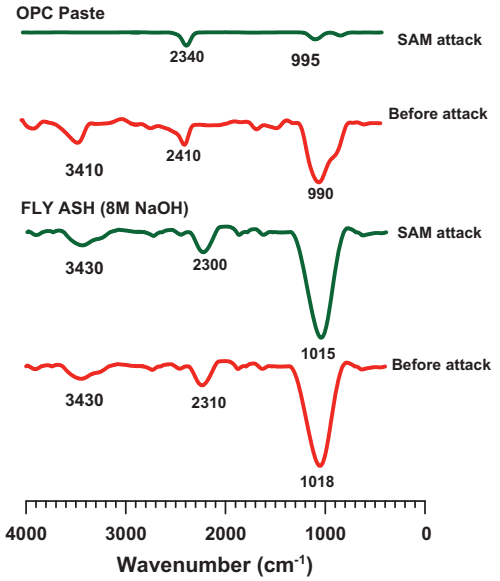

Fig. 11. FTIR spectra of a 28 day old OPC paste and a heat cured (75 °C for 48 h) 8 M NaOH activated fly ash paste, before and after salicylic acid–methanol (SAM) attack.

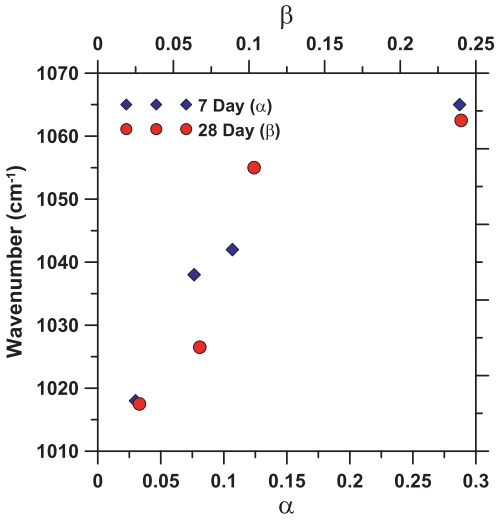

Fig. 12. Wavenumber of the major Si–O–Si stretching vibration signal as a function of compositional coefficients.

associated with the main Si–O–Si peak after the attack. This sample also resulted in the highest amount of insoluble residue after the SAM attack. This could be construed as an indication of the fact that phases that are not susceptible to the SAM attack are formed. The fact that the spectra remain virtually unchanged before and after the SAM attack indicates that the FTIR signatures of pastes with higher alkalinities are dominated by the signals for the silica-rich gel. The FTIR spectra of the pastes before and after the SAM attack provide an illustration of the influence of alkalinity of the powder activators in bringing about modifications in the reaction products.

3.5. Reaction products and compressive strength

A comparison of Fig. 8a and b shows that the asymmetric stretching vibration peak of Si–O–Si shifts to higher wavenumbers for pastes having a higher n value, suggesting increased Si polymerization in the sodium silicate gel. Moreover, this gel is denser, which explains the higher compressive strengths for the high n value mixtures at all ages. Accelerated chloride transport tests have shown that the transport parameters (rapid chloride permeability or the non-steady state migration coefficients) of these binders at 28 days of curing are consistently lower than those of OPC mixtures (w/c of 0.40) cured for 56 days, providing further evidence of a denser microstructure. When the 28-day FTIR spectra of the pastes of a certain n value are considered, the wavenumbers of the dominant band increases slightly with increasing M_s. This is in agreement with the 28 day compressive strength values, which also increases slightly with M_s as can be observed in Fig. 6a–c. However, when the 7-day spectra are considered, higher M_s is seen to shift the dominant band to a lower wavenumber, indicating reduced polymerization (or cross-linking), and consequently lower strengths with increasing M_s as shown in Fig. 6a–c. This indicates that at higher M_s values, time-dependent increase in silica polymerization is occurring. These trends in wavenumbers can thus be related to the compositional coefficients, α and β, which were found to relate well to the early (3 and 7 day) and later (14 and 28 day) age compressive strengths as was shown in Fig. 7. Fig. 12 shows the relationship between α and the wavenumbers of the Si–O–Si stretching peak at 7 days, and between β and the wavenumbers of the peak at 28 days. Increasing amounts of Q^3 silicon entities or increased polymerization in C–S–H gel leading to increase in chain lengths or more cross-linking, exhibited through an increase in wavenumber, has been reported to somewhat enhance the mechanical properties [33,40]. Better mechanical properties have also been attributed to the presence of a sodium silicate gel with SiO_2/Na_2O of 5 or more [23].

Between 7 and 28 days of curing, there is a general increase in peak wavenumber shifts, with the highest shift observed for the mixtures with higher M_s values, as shown in the lower panels of Fig. 8a and b, attributable to increased silica polymerization with time as explained earlier. Such increase in wavenumber with hydration time is also seen in the case of ordinary Portland cements [41]. This trend is also in line with the compressive strength results where the binders activated using a high M_s activator showed strength gain between 7 and 28 days, whereas the one activated using a lower M_s did not show appreciable strength gain in this period. For a given n value, binders with low M_s activators demonstrate significant early age strength development, but the later age strength development is relatively insignificant as can be observed from Fig. 6a–c.

4. Conclusions

The influence of the powder activator characteristics on the strength and reaction products of activated slag binders are reported in this study. The following conclusions are arrived at based on this research.

- Higher levels of alkalinity (i.e., higher values of Na_2O-to-source material ratio (n)) resulted in higher peak temperatures and increased early and later age compressive strengths for powder sodium silicate + NaOH activated slag binders. At the chosen n values, a strength reduction was observed with an increase in activator modulus (M_s) at early ages (3 and 7 days), and a slight strength increase at later ages (14 and 28 days). A careful selection of the activator parameters (n and M_s) along with use of powder activators can provide compressive strengths in the 20–30 MPa range, which is appropriate for many concrete applications.
- Compositional coefficients, α and β, which are functions of n and M_s were used, that relate well to the early and later age strength development respectively in alkali powder activated slag binders. In addition, these coefficients were also found to

correspond to the trends in wavenumbers of the Si–O–Si stretching vibration with age for mixtures with different n and activator M_s values.

- The wavenumbers corresponding to the Si–O–Si stretching vibrations were found increase with the curing time. The characteristic peaks appeared at wavenumbers between 1018 and 1065 cm^{-1} depending on the activator alkalinity and the moist curing duration. This is much higher than the 950–1000 cm^{-1} range that is typical of C–S–H gels from OPC hydration where the silicates are less polymerized. Possible reasons for such an observation have been outlined, constructed around changes in C–S–H gel and/or the presence of a silica rich gel that shifts the Si–O–Si stretching vibration to higher wavenumbers. It is shown that lower alkalinity (n = 0.05 and M_s = 1.5) resulted in the formation of a low Ca/Si ratio C–S–H gel as the dominant reaction product while higher alkalinity (n = 0.25 and M_s = 0.6) resulted in the formation of additional silica rich gel as observed from the micrographs.
- Salicylic acid–methanol (SAM) attack on the binder pastes confirmed the alkali silicate powder activation induced modifications in the reaction products. The paste of highest alkalinity (and the highest strength) showed virtually no change in the main Si–O–Si peak after the SAM attack, implying the formation of a silica-rich gel as one of the dominant reaction products. The FTIR spectra for the highly alkaline mixtures were indicative of the sodium silicate gel that was formed. In contrast, the main Si–O–Si peak in the lowest alkalinity paste was virtually non-existent after the SAM attack, indicating the potential formation of a phase similar to the conventional C–S–H gel.

Acknowledgements

The authors sincerely acknowledge the funding from New York State Energy Research and Development Authority (NYSERDA) towards the conduct of this study. The materials were supplied by Holcim US and PQ Corporation, which is gratefully acknowledged. The contents of this paper reflect the views of the authors who are responsible for the facts and accuracy of the data presented herein, and do not necessarily reflect the views and policies of the funding agency, nor do the contents constitute a standard, specification, or a regulation.

References

[1] Yang KH, Song JK, Ashour AF, Lee ET. Properties of cementless mortars activated by sodium silicate. Constr Build Mater 2008;22:1981–9.
[2] Brough AR, Atkinson A. Sodium silicate-based, alkali-activated slag mortars: Part I. Strength, hydration and microstructure. Cem Concr Res 2002;32:865–72.
[3] Chang JJ. A study on the setting characteristics of sodium silicate-activated slag pastes. Cem Concr Res 2003;33:1005–11.
[4] Silva PD, Crenstil KS, Sirivivatnanon V. Kinetics of geopolymerization: role of Al_2O_3 and SiO_2. Cem Concr Res 2007;37:512–8.
[5] Duxson P, Provis JL, Lukey GC, Mallicoat SW, Kriven WM, van Deventer JSJ. Understanding the relationship between geopolymer composition, microstructure and mechanical properties. J Colloids Surf A: Physiochem Eng Aspects 2005;269:47–58.
[6] Ravikumar D, Peethamparan S, Neithalath N. Structure and strength of NaOH activated concretes containing fly ash or GGBFS as the sole binder. Cem Concr Compos 2010;32:399–410.
[7] Bakharev T, Sanjayan JG, Cheng YB. Alkali activation of Australian slag cements. Cem Concr Res 1999;29:113–20.
[8] Shi C, Yinyu L. Investigation on some factors affecting the characteristics of alkali-phosphorus slag cement. Cem Concr Res 1989;19:527–33.
[9] Krizan D, Zivanovic B. Effects of dosage and modulus of water glass on early hydration of alkali-slag cements. Cem Concr Res 2002;32:1181–8.
[10] Oh JE, Monteiro PJM, Jun SS, Choi S, Clark SM. The evolution of strength and crystalline phases for alkali-activated ground blast furnace slag and fly ash-based geopolymers. Cem Concr Res 2010;40:189–96.
[11] Wang SD, Scrivener KL. ^{29}Si and ^{27}Al NMR study of alkali-activated slag. Cem Concr Res 2003;33:769–74.
[12] Shi C, Day RL. Pozzolanic reaction in the presence of chemical activators: Part II—Reaction products and mechanism. Cem Concr Res 2000;30:607–13.
[13] Shi C, Day RL. Some factors affecting early hydration of alkali-slag cements. Cem Concr Res 1996;26:439–47.
[14] Fernández-Jiménez A, Palomo JG, Puertas F. Alkali-activated slag mortars: mechanical strength behavior. Cem Concr Res 1999;29:1313–21.
[15] Wang SD, Scrivener KL. Hydration products of alkali activated slag cement. Cem Concr Res 1995;25:561–71.
[16] Richardson IG, Cabrera JG. The nature of C–S–H in model slag-cements. Cem Concr Compos 2000;22:259–66.
[17] Song S, Jennings HM. Pore solution chemistry of alkali-activated ground granulated blast-furnace slag. Cem Concr Res 1999;29:159–70.
[18] Bakharev T, Sanjayan JG, Cheng YB. Sulfate attack on alkali-activated slag concrete. Cem Concr Res 2002;32:211–6.
[19] Jawed I, Skalny J. Alkalies in cement: A review: II. Effect of alkalies on hydration and performance of Portland cement. Cement Concr. Res 1978;8:37–51.
[20] Schwarz N, DuBois M, Neithalath N. Electrical conductivity based characterization of plain and coarse glass powder modified cement pastes. Cem Concr Compos 2007;29:656–66.
[21] McCarter WJ, Garvin S, Bouzid N. Impedance measurements on cement paste. J Mater Sci Lett 1988;7:1056–7.
[22] Garcia Lodeiro I, Fernández-Jiménez A, Blanco MT, Palomo A. FTIR study of sol–gel synthesis of cementitious gels: C–S–H and N–A–S–H. J Sol–Gel Sci Technol 2008;45:63–72.
[23] Dimas D, Giannopoulou I, Panias D. Polymerization in sodium silicate solution: a fundamental process in geopolymerization technology. J Mater Sci 2009;44:3719–30.
[24] Shi C, Krivenko PV, Roy D. Alkali-activated cement and concretes. New York: Taylor and Francis; 2006.
[25] Altan E, Erdoğan ST. Alkali activation of slag at ambient and elevated temperatures. Cem Concr Compos 2012;34:131–9.
[26] Yip CK, Lukey GC, van Deventer JSJ. The coexistence of geopolymeric gel and calcium silicate hydrate at the early stage of alkaline activation. Cem Concr Res 2005;35:1688–97.
[27] Song S, Sohn D, Jennings HM, Mason TO. Hydration of alkali-activated ground granulated blast furnace slag. J Mater Sci 2000;35:249–57.
[28] Ben Haha M, Le Saout G, Winnefeld F, Lothenbach B. Influence of activator type on hydration kinetics, hydrate assemblage and microstructural development of alkali-activated blast furnace slags. Cem Concr Res 2011;41:301–10.
[29] Bernal SA, de Gutiérrez RM, Pedraza AL, Provis JL, Rodriguez ED, Delvasto S. Effect of binder content on the performance of alkali-activated slag concretes. Cem Concr Res 2011;41:1–8.
[30] Palomo A, Fernández-Jiménez A, Kovalchuk G, Ordoñez LM, Naranjo MC. OPC-fly ash cementitious systems: study of gel binders produced during alkaline hydration. J Mater Sci 2007;42:2958–66.
[31] García Lodeiro I, Macphee DE, Palomo A, Fernández-Jiménez A. Effect of alkalis on fresh C–S–H gels. FTIR analysis. Cem Concr Res 2009;39:147–53.
[32] Palacios M, Puertas F. Effect of carbonation on alkali-activated slag paste. J Am Ceram Soc 2006;89:3211–21.
[33] Fernández-Jiménez A, Puertas F, Sobrados I, Sanz J. Structure of calcium silicate hydrates formed in alkaline-activated slag: influence of the type of alkaline activator. J Am Ceram Soc 2003;86:1389–94.
[34] Schneider J, Cincotto MA, Panepucci29 Si H. ^{29}Si and ^{27}Al high-resolution NMR characterization of calcium silicate hydrate phases in activated blast-furnace slag pastes. Cem Concr Res 2001;31:993–1001.
[35] Macphee DE, Luke K, Glasser FP, Lachowski EE. Solubility and ageing of calcium silicate hydrates in alkaline solutions at 25 C. J Am Ceram Soc 1989;72(4):646–54.
[36] Puertas F, Fernández-Jiménez A, Varela MTB. Pore solution in alkali-activated slag cement pastes. Relation to the composition and structure of calcium silicate hydrate. Cem Concr Res 2004;34:139–48.
[37] García Lodeiro I, Fernández-Jiménez A, Palomo A, Macphee DE. Effect on fresh C–S–H gels of the simultaneous addition of alkali and aluminium. Cem Concr Res 2010;40:27–32.
[38] Mitchell LD, Margeson JC, Beaudoin JJ. Synthesis and characterisation of lithium and sodium doped C–S–H. In: 12th International congress on the chemistry of cement, Montreal; July 8–13, 2007; p. 1–17.
[39] Falcone JS, Bass JL, Angelella M, Schenk ER, Brensinger K. The determination of sodium silicate composition using ATR FT-IR. Ind Eng Chem Res 2010;49:6287–90.
[40] Sakulich AR, Miller S, Barsoum MW. Chemical and microstructural characterization of 20 month old alkali activated slag cements. J Am Ceram Soc 2010;93(6):1741–8.
[41] Ramachandran VS, Haber JJ. Handbook of analytical techniques in concrete science and technology: principles, techniques and applications. New York: William Andrew; 2001.